Stability, Miscoding Potential, and Repair of 2′-Deoxyxanthosine in DNA: Implications for Nitric Oxide-Induced Mutagenesis†

Gerald E. Wuenschell,‡ Timothy R. O'Connor,# and John Termini*,‡

Division of Molecular Biology, Division of Biology, Beckman Research Institute of the City of Hope, 1450 East Duarte Road, Duarte, California 91010

Received August 28, 2002

ABSTRACT: Nitric oxide (NO•) reacts with guanine in DNA and RNA to produce xanthine (X) as a major product. Despite its potential importance in NO•-mediated mutagenesis, the biochemical properties of X in polynucleotides have been relatively unexplored. We describe the synthesis and chemical characterization of xanthine-containing oligonucleotides and report on the susceptibility of X to depurination, its miscoding potential during replication by polymerases, and its recognition and excision by several members of the base excision repair (BER) family of DNA glycosylases. At neutral pH, X was found to be only slightly less stable than guanine to depurination ($k_X/k_G = 1.19$), whereas at pH ≤ 4 the depurination rate exceeded that of G by more than an order of magnitude. HIV-1 RT inserted dCTP and dTTP with approximately equal frequencies opposite X in a DNA template, whereas DNA Pol 1(KF⁻) preferentially inserted dCTP. Several DNA glycosylases were found to excise X specifically in X•C base pairs, whereas activity toward X•G, X•A, or X•T pairs was detected only for AlkA. The order of reactivity of glycosylases for the removal of X•C base pairs was found to be AlkA > Mpg > Nth > Fpg. Implications of these results for the induction of mutations by nitric oxide are discussed.

The deamination of bases in DNA and RNA is of great interest owing to the mutation inducing potential resulting from changes in hydrogen bonding arrangements. The hydrolytic deamination of cytosine and methylcytosine has been extensively studied (*1*−*4*). The half-life for the spontaneous hydrolytic deamination of C at 37 °C in dsDNA has been estimated to be approximately 30 000 years (*4*). The hydrolytic deamination of purines, however, occurs at a rate that is at least an order of magnitude slower (*5*), and thus consideration of only the hydrolysis rates would suggest that the occurrence of xanthine (X)[1] or hypoxanthine (hX) in DNA would be extremely small. However, purine deamination may also occur via the action of nitric oxide (NO•) and other nitrosating agents through an oxidative mechanism (*6*−*9*). Nitric oxide reacts with molecular oxygen to form the powerful nitrosating agent dinitrogen trioxide (N_2O_3). Nitrosation, followed by protonation and a series of elimination reactions, leads to the formation of an N2-diazonium intermediate. The corresponding guanine-derived intermediate is thought to undergo ring-opening at C1−C5 with concomitant elimination of N2, followed by hydrolysis and rearrangement to provide xanthine (*8*, *9*).

Scheme 1: Deprotonation at N3 of X (pK ∼ 5.5) Leads to the Stable Enolate

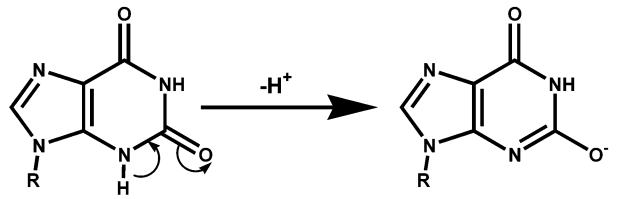

Xanthine is an unusual nucleic acid base in that it exists as a stable enolate at physiological pH, as shown in Scheme 1 (*10*, *11*). Xanthine in DNA under acidic conditions is known to be unstable to depurination (*12*, *13*); however, its stability at neutral pH has not been determined directly. To circumvent the formation of abasic sites during the nitrous acid induced deamination of 2′-deoxyguanosine, Moschel and Keefer described the synthesis of 2′-deoxyxanthosine using sodium nitroprusside under alkaline conditions (*14*). The synthesis of the O^6-NPE protected phosphoramidite of 2′-deoxyxanthosine and the preparation of oligonucleotides containing this base has been described (*15*). Attempts to prepare oligonucleotides from the corresponding phosphotriester was reported to result in the formation of "side products" (*16*). Van Aerschot et al. have described the preparation of O^2,O^6-(bis)NPE protected 2′-deoxyxanthosine and the corresponding phosphotriester (*16*). The preparation of the analogous phosphoramidite has been reported, but no details of the synthetic procedure nor spectral characterization of any intermediates were provided (*17*).

† Supported by NIH Grant GM59219 and GM53962 to J.T.

* To whom correspondence should be addressed. Phone: (626) 301−8169. FAX: (626) 301−8271. E-mail: jtermini@coh.org.

‡ Division of Molecular Biology.

Division of Biology.

[1] Abbreviations: BER, base excision repair; X, xanthine; hX, hypoxanthine; NPE; 4-nitrophenylethyl; DMT, 4-4′-dimethoxytrityl; DBU, 1,8-diazabicyclo[5.4.0]undec-7-one; DNA Pol 1(KF⁻), large fragment of DNA polymerase I exonuclease-free Klenow enzyme (recombinant); HIV-1-RT, human immunodeficiency virus I reverse transcriptase (recombinant); AlkA, 3-methyladenine DNA glycosylase II; Mpg, *N*-methylpurine DNA glycosylase; Nth, endonuclease III; Fpg, formamidopyrimidine DNA glycosylase.

10.1021/bi0205597 CCC: $25.00
Published on Web 03/07/2003

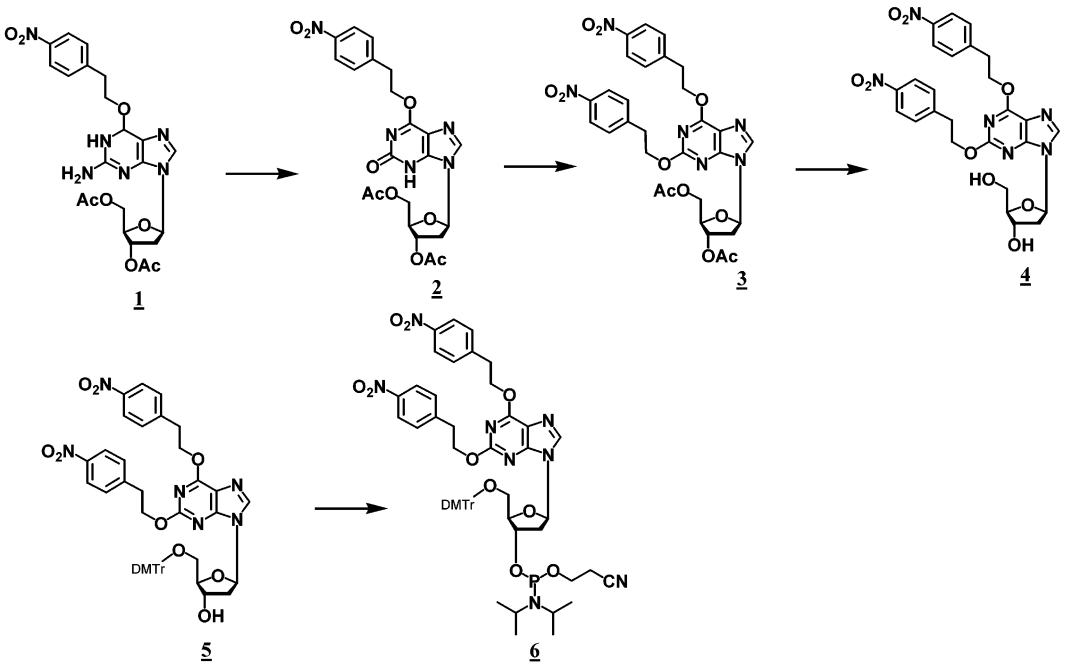

FIGURE 1: Synthetic route used to prepare the phosphoramidite of 2′-deoxyxanthosine.

We describe the preparation of this material, as well as details for incorporation into oligodeoxynucleotides. The stability of xanthine in DNA was evaluated over a range of pH values. The pH-dependent rates of depurination reconcile the apparent paradox of xanthine instability with quantitative descriptions of its abundance in NO•-treated DNA. The base coding properties of xanthine in template DNA were evaluated by studying the steady-state kinetics for the insertion of dNTPs by HIV reverse transcriptase (HIV-1RT) and DNA polymerase I (KF^-). Finally, the ability of several DNA glycosylases to recognize and remove xanthine from X•N base pairs in DNA was determined.

MATERIALS AND METHODS

Materials. 2′-Deoxyguanosine was purchased from Chem-Impex International (Dale Wood, IL). Chromatography was carried out using Silica Gel H from Fluka (Milwaukee, WI). Phosphoramidites and oligonucleotide synthesis reagents were purchased from Glen Research (Sterling, VA). Radioisotopic reagents were purchased from ICN Radiochemicals (Costa Mesa, CA). DNAPol1(KF^-) was purchased from USB Corporation (Cleveland, OH) and had a specific activity of 20 000 units per milligram. HIV-1-RT (*19*) and BER enzymes (*36*) were isolated as previously described. Other reagents and solvents were purchased from Aldrich (Milwaukee, WI), J. T. Baker (Philipsburg, NJ), or Fisher (Tustin, CA). Radioactive gels were imaged and analyzed using a Molecular Dynamics PhosphorImager running ImageQuant software purchased under NSF Grant BIR-9220534.

Synthesis of the Phosphoramidite of 2′-Deoxyxanthosine. The synthetic scheme for the preparation of the phosphoramidite of 2′-deoxyxanthosine (Figure 1) follows the general outline of Van Aerschot for synthesis of the phosphotriester (*16*). Modifications to the methodology described for O^2,O^6-bis-protected 4-nitrophenyl ethers of xanthine nucleosides are presented that delete several chromatographic steps and improve the isolated yields allowing for more practical preparative synthesis of oligonucleotides.

2,6-di-O-[2-(4-Nitrophenyl)ethyl]-2′-deoxyxanthosine (***4***). A solution of 6-*O*-[2-(4-nitrophenyl)ethyl]-3′,5′-diacetyl-2′-deoxyguanosine (**1**), prepared as described by Van Aershot et al., (1.48 g, 2.96 mmol) was dissolved in acetone (6 mL). Sodium nitrite (4.44 g, 64 mmol) was dissolved separately in water (13 mL). The two solutions were then mixed and glacial acetic acid (6.5 mL) was added, resulting in immediate gas evolution. The reaction mixture was monitored by silica gel TLC using 5% methanol in dichloromethane as eluent. Reaction was nearly complete after 1 h, as indicated by the disappearance of the starting material ($R_f = 0.52$), the appearance of a major product ($R_f = 0.35$), and some minor higher R_f compounds ($R_f = 0.63-0.74$). The reaction mixture was poured into a separatory funnel containing ethyl acetate (50 mL) and washed with saturated sodium bicarbonate (150 mL). The organic phase was dried over anhydrous sodium sulfate, filtered, concentrated to an oil on a rotary evaporator, redissolved in benzene (30 mL), and lyophilized on a vacuum line. The crude acetylated, mono-NPE-protected deoxyxanthosine (**2**) was used in subsequent steps without further purification. The second NPE group was introduced by placing lyophilized **2** into an oven-dried flask and adding 4-nitrophenylethanol (1.51 g, 9.03 mmol), triphenylphosphine (2.37 g, 9.04 mmol), and dry dioxane (25 mL) under argon. The mixture was then frozen in dry ice and relyophilized to remove any trace water. The residue was redissolved in dry dioxane (30 mL) under argon and diethylazidodicarboxylate (1.5 mL, 9.53 mmol) was added via a gastight syringe. TLC (silica gel), eluting with 20% acetone in chloroform, showed that the reaction was complete after 2.5 h, indicated by the disappearance of the starting material ($R_f = 0.29$) and the appearance of a new major spot ($R_f = 0.71$). Water (0.5 mL) was added and the mixture was stirred for 60 min. The reaction mixture was then frozen and lyophilized to provide **3**. Deacetylation was carried out without further purification. Lyophilized **3** was dissolved in methanol (25 mL) and 28−30% aqueous ammonia (20 mL) was added with stirring. After 6.5 h, the reaction mixture was evaporated to an oil

then resuspended in 40 mL of diethyl ether. After stirring for 30 min, the mixture was transferred to a centrifuge tube and the ether insoluble salts were pelleted. This procedure was repeated until the supernatant exhibited no detectable color. The product (**4**) was vacuum-dried. TLC on silica gel using 5% MeOH/CH_2Cl_2 exhibited a single major spot (R_f = 0.36). Yield, 1.26 g (FW 560.53, 2.25 mmol, 76% from **1**). ^{1}H NMR (DMSO-d_6, 300 MHz) δ 8.35 (s, 1 H, C-8), 8.20−8.14 (2xd, 4 H, NPE-*ortho*), 7.65−7.59 (2xd, 2 H, NPE-*meta*), 6.29 (m, 1 H, C-1′), 5.33 (d, 1 H, C-3′-OH), 4.94 (t, 1 H, C-5′-OH), 4.76 (t, 2 H, NPE-O−CH_2), 4.60 (t, 2 H, NPE-O−CH_2), 4.40 (m, 1 H, C-4′), 3.85 (m, 1 H, C-3′), 3.63−3.45 (m, 2 H, C-5′), 3.31−3.19 (m, 4 H, NPE-Ar-CH_2), 2.69 (m, 1 H, C-2′), 2.27 (m, 1 H, C-2′)

5′-O-(4,4′-Dimethoxytrityl)-2,6-di-O-[2-(4-nitrophenyl)-ethyl]-2′-deoxyxanthosine (**5**). A dry 50 mL flask was charged with **4** (1.25 g, 2.21 mmol) and 4,4′-dimethoxytrityl chloride (1.50 g, 4.43 mmol) under an argon atmosphere. Dry pyridine (25 mL) was added via a gastight syringe and the reaction mixture stirred under argon until judged complete by TLC (3% MeOH/CH_2Cl_2) with the appearance of a new product at R_f 0.76 (17 h). Methanol (1 mL) was added to the reaction mixture and stirred for an additional 1.5 h. The reaction mixture was dissolved in ethyl acetate (100 mL), transferred to a separatory funnel, and washed once with 1% sodium bicarbonate (100 mL) and twice with water (100 mL each). The organic phase was dried over anhydrous sodium sulfate, filtered, and concentrated on a rotary evaporator. The residue was dissolved in a minimal amount of dichloromethane containing 0.5% pyridine and loaded onto a 20 mm column packed with silica gel (50 mL dry volume) slurried in 0.5% pyridine in diethyl ether. The column was eluted with 0.5% pyridine in diethyl ether (150 mL) followed by 100 mL aliquots of diethyl ether containing 2.5, 3, and 4% MeOH. The eluent was collected in 20−25 mL fractions. TLC of the fractions on silica gel, eluting with 3% methanol in dichloromethane, indicated that the product eluted in fractions 11−13. The combined eluates containing the product were concentrated to dryness on a rotary evaporator, redissolved in 50 mL of benzene, frozen, and lyophilized on a vacuum line to remove solvents and pyridine to provide **5** as a pale yellow solid. Yield (**5**), 0.85 g (FW 868.90, 0.979 mmol, 44.23%). ^{1}H NMR (DMSO-d_6, 300 MHz) δ 8.26 (s, 1 H, C-8), 8.19−8.12 (2xd, 4 H, NPE-*ortho*), 7.67−7.11(m, 17 H, DMT-Ar), 6.78−6.67 (2xd, 2 H, NPE-*meta*), 6.34 (t, 1 H, C-1′), 5.38 (d, 1 H, C-3′-OH), 4.75 (t, 2 H, NPE-O-CH_2), 4.57−4.35 (m, 3 H, NPE-O-CH_2 + C-4′), 3.97 (m, 1 H, C-3′), 3.69 (s, 3 H, DMT-methyl), 3.68 (s, 3 H, DMT-methyl), 3.27 (t, 2 H, NPE-Ar-CH_2), 3.25−3.05 (m, 2 H, C-5′), 3.15 (t, 2 H, NPE-Ar-CH_2), 2.87 (m, 1 H, C-2′), 2.33 (m, 1 H, C-2′).

5′-O-(4,4′-Dimethoxytrityl)-2,6-di-O-[2-(4-nitrophenyl)-ethyl]-2′-deoxyxanthosine-3′-O-(N,N-diisopropylamino-cyanoethoxy) phosphoramidite (**6**). **5** (110 mg, 127 μmol) was dissolved in 2 mL of dry benzene and 287 μmol of dry triethylamine in a 15 × 45 mm vial to which had been added several freshly activated 4 Å molecular sieves. The vial was capped with a septum, and the resulting mixture was dried by stirring under positive nitrogen pressure for 16 h. 2-Cyanoethyl diisopropylchlorophosphoramidite (35 μL, d 1.061, FW 236.68, 157 μmol) was added via a gastight syringe. The mixture was allowed to react for a total of 24 h. Silica gel TLC using 6:4 cyclohexane/dichloromethane containing 2% triethylamine as eluant revealed diastereomeric separation of the products, eluting at R_f = 0.17 and 0.25. The reaction mixture was filtered through a 0.22μ PTFE syringe filter into a dried DNA synthesizer vial. The clear, light yellow filtrates were lyophilized to dryness and used without further purification. Yield (**6**) 125 mg, 117 μmol, 92% from (**5**). ^{1}H NMR (acetonitrile-d_3, 360 MHz) δ 8.14−8.09(2xd, 4 H, NPE-*ortho*), 7.95 (s, 1 H, C-8), 7.75−7.10 (m, 13 H, DMT-Ar), 6.75−6.65 (2 × 2xd, 2 H, NPE-*meta*), 6.29 (2xt, 1 H, C-1′), 4.76 (t, 2 H, NPE-O−CH_2), 4.20−4.08 (m, 3 H, NPE-O-CH_2 + C-4′), 3.78−3.42 (m, 3 H, C-3′ +CE-OCH_2), 3.70 (2 × 2xs, 6 H, DMT-methyl), 3.68 (s, 3 H, DMT-methyl), 3.27 (t, 2 H, NPE-Ar-CH_2), 3.25−3.05 (m, 2 H, C-5′), 3.01(m, 2 H, *i*Pr-CH), 3.15 (t, 2 H, NPE-Ar-CH_2), 3.25 (m, 1 H, C-2′), 2.61(t, 1H, CE-CH_2CN), 2.49 (t, 1H, CE-CH_2CN), 1.66 (m, 1 H, C-2′). The region from 1.45 to 0.85 ppm includes the isopropyl methyl groups, but also the methyl groups from excess triethylamine (and its hydrochloride) from the reaction mixture as well as the triethylamine added to the NMR solvent to stabilize the product. ^{31}P NMR (acetonitrile-d_3, 360 MHz) δ 149.58 (s, br).

Synthesis of Oligonucleotides Containing Deoxyxanthosine. Lyophilized phosphoramidite (**6**) was dissolved in dry acetonitrile (10 μL/mg), to yield a 0.1 M solution. Freshly activated 4 Å molecular sieves were added prior to loading onto a Pharmacia Gene Assembler DNA synthesizer. DNA synthesis was conducted on 0.2 μM scale. Coupling yields for (**6**) were typically ∼95%. Xanthine-containing oligos were then synthesized in the trityl-off mode without any further modification of the standard procedures. Oligos were cleaved from the support by heating at 50 °C for 16 h in 30% aqueous ammonia. Ammonia was removed by drying under a stream of N_2.

The NPE-protecting groups were removed in a separate step. The sample was redissolved in 2.5 mL of dry pyridine to which 500 μL of DBU were added with stirring. The mixture was allowed to stir under dry nitrogen for 18 h at room temperature. The volume was reduced to ∼0.5 mL under dry nitrogen, then 5 mL of diethyl ether and 3 mL of 3% aqueous ammonia were added. After mixing, the aqueous phase was drawn off and the organic phase extracted with a second 3 mL portion of 3% aqueous ammonia. The combined aqueous phases were lyophilized, transferred to a tare-weighed vial with several small portions of water, and the frozen stock solution stored at −80 °C until needed.

400 μL of the stock solution was diluted with 400 μL of formamide and purified on a 1.4 mm, 15% PAGE/8 M urea gel. Product oligonucleotide was visualized by UV-shadowing and recovered from the excised band via electroelution using an Elutrap (Schleicher & Schuell) followed by Sephadex G25 desalting. The concentration was determined by UV spectroscopy (*18*). The extinction coefficient for guanine was used to calculate the contribution of xanthine (values within 10% at neutral pH). The composition of oligos containing xanthine was verified by HPLC integration of nucleobases produced by formic acid hydrolysis. A sample (10 μL of 200 μg/μL, 165 nmol) of oligonucleotide was hydrolyzed by the addition of 40 μL of 96% formic acid followed by heating at 80 °C for 1 h. 50 μL of this solution was injected onto a Beckman Ultrasphere ODS C18 column (4.6 × 250

mm) using an isocratic buffer consisting of 2% MeOH in 25 mM NH_4PO_4 (pH = 6.0) on a Hewlett-Packard 1100 HPLC system. Direct area ratios from the chromatogram, measured at 268 nm, were consistent with expected G:X:A stoichiometries. The retention times for G, X, and A using these chromatographic conditions were 5.7, 6.3, and 12.8 min, respectively. The molecular weight of xanthine containing oligonucleotides was verified by MALDI-TOF using a Voyager mass spectrometer (Perseptive Biosystems). As a typical example, the calculated/observed mass (M+1) for oligo T3 was found to be 10272.7/10271.4. The sequences of all oligonucleotides used in these studies are provided in Figure 2.

Depurination Rate Measurements in DNA. The xanthine depurination rate as a function of pH was determined for single-stranded oligonucleotide T3. The depurination rate for a guanine residue in an identical sequence environment (oligonucleotide T4) was also measured. Depurination reactions were carried out in 0.1 M NaCl/0.01 M phosphate/0.01 M citrate (*2*), over a pH range of 4−7 adjusted by NaOH addition. To 100 μL of 2× buffer was added 1 μL of 10 μM unlabeled oligonucleotide stock solution, and 10−15 cpm of ^{33}P-labeled oligonucleotide (1−5 μL, ∼1−5% of unlabeled oligo). Volume was brought to 200 μL with distilled water, and reactions were sealed and incubated at 70 °C. Two 10 μL samples were removed from each reaction at various time points. A total of 10 μL of 2.0 M piperidine was added to each; reactions were incubated for 30 min at 50 °C, then evaporated to dryness. Samples were dissolved in 5 μL of loading dye (90% formamide containing 20 mM EDTA and 0.05% each of xylene cyanol and bromophenol blue) and run on a 15% PAGE gel containing 8 M urea. Oligonucleotide cleavage patterns were analyzed using a Molecular Dynamics PhosphorImager with ImageQuant software. The rate of decay of the signal corresponding to full-length oligonucleotide (F) can be described by eq 1.

$$-\frac{\partial[F]}{\partial t} = (k_1 + k_2 + k_3 ... + kN)[F] \qquad (1)$$

Here $k_{1...n}$ represents the rate constants for depurination/depyrimidination for bases at positions 1 through *n*. Rearrangement and integration provide the expression shown in eq 2.

$$\ln\frac{[F_0]}{[F]} = (k_1 + k_2 + k_3 ... + k_N)t \qquad (2)$$

Since $[F] \propto [I]$, the integrated gel band intensity, a plot of $\ln I_0/I$ vs time generates a plot with a slope of $(k_1 + k_2 + k_3 ... + k_N)$. Under the conditions used, little depyrimidination was observed, and depurination occurred nearly exclusively at G and X. The depurination rate of X in oligo T3 was compared directly to that of G in an identical sequence environment (oligo T4). Values determined are presented in Table 1. Rate constants *k* represent the mean value of three separate determinations

Steady-State Kinetics of dNTP Incorporation Opposite Xanthine in DNA by HIV-1 RT and DNA Pol1(KF$^-$). 2× stock solutions of primer/template/enzyme were made up in a total volume of 100 μL. These stock solutions were 300 nM in oligonucleotide templates (T3 or T4). The unlabeled

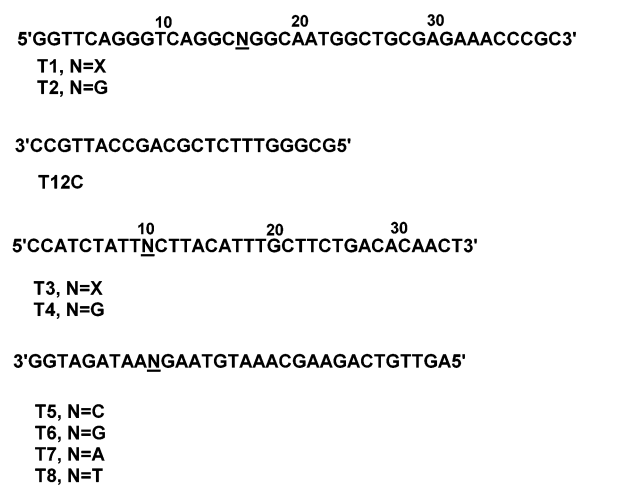

FIGURE 2: Substrate oligonucleotides used in these studies.

Table 1: Rate Constants for Depurination of X and G in DNA

	pH 4	pH 5	pH 6	pH 7
$k(X)_{10}$[a]	199± 9[b]	8.11 ± 0.8	0.578 ±0.008	0.108 ±0.0012
$k(G)_{10}$	14.0 ± 1.4	2.47 ± 0.2	0.135 ± 0.010	0.090 ±0.00098
$k(X)_{10}$/ $k(G)_{10}$	14.3	3.28	4.28	1.19

[a] Units of *k* are s^{-1}. [b] All values of *k* and SD × 10^{-6}.

primer concentration was 200 nM. A total of 1−8 μL of 5′ γ-^{33}P end-labeled primer was added to the reactions (final concentration ≤ 10% of the unlabeled primer). The annealing of primer/template strands was accomplished by incubating at 90 °C for 5−10 min in a heat block followed by cooling to ≤ 40 °C. Buffers for either DNA Pol1(KF$^-$) or HIV-1RT were then added. Extension reactions carried out with HIV-1RT were supplemented with 4 μL 1 M KCl and 1 μL 200 mM DTT. Polymerase enzymes (10 μL of 0.1 U/μL for Klenow fragment or 25 μL of 1.0 μM for HIV-RT) were added to the annealed template/primer solution. Total reaction volume for the primer/template/enzyme solutions was 100 μL. Stock solutions of each dNTP were prepared at 2× the final reaction concentration. Final concentrations were between 50 μM and 1 mM; typically six to eight concentrations were chosen within this range. Reactions were initiated by adding 4 μL of 2× dNTP solution to 4 μL of primer/template/enzyme solution at 37 °C. Reactions were allowed to proceed for a time within the linear phase (∼5′) and were quenched with 16 μL of a stop solution consisting of 90% formamide and 20 mM EDTA. Primer extension results were analyzed and steady state kinetic constants were obtained as previously described (*19*).

BER Enzyme Assays. Reaction buffer (5×) for Fpg, Mpg, and Nth enzymes consisted of 350 mM Tris, 200 μM EDTA, 500 mM KCl, 50 μM β-mercaptoethanol, and 25% glycerol, pH = 7.5−8.0. Buffer for AlkA reactions omitted KCl. ^{32}P end-labeled xanthine containing oligonucleotide T3 (1 μL, 0.2 pmol) was separately annealed to each of the T5-T8 complements (1 μL, 1 pmol) in a total volume of 17.5 μL (10.5 μL of water, 5 μL of 5× buffer) to form duplexes containing all possible X·N base pairs. BER enzymes were stored as 50 μM stock solutions. To initiate BER, 5 pmol of Mpg, Nth, Fpg, or AlkA in 7.5 μL were added. Reactions were incubated at 37 °C for 2 h. Final reaction stoichiometry was 8 nM of X containing duplex and 200 nM of BER

enzyme. For reactions with BER enzymes possessing only glycosylase but not AP lyase activity (Mpg, AlkA) NaOH hydrolysis (5 μL of 1.2 M NaOH, 60 °C for 30 min) was carried out to cleave potential abasic sites. Reactions were stopped by the addition of 6 μL of loading buffer, heating to 70 °C for 10 min, then quick cooling on ice. Aliquots were analyzed by PAGE (20% acrylamide, 7 M urea) and cleavage patterns were imaged and analyzed using the Phosphorimager. Haynes plots for the reaction of Mpg with the T3·T6 duplex were carried out as previously described (*20*).

RESULTS

Synthesis of X Phosphoramidites and Oligonucleotides. The synthesis of oligonucleotides containing xanthine was originally described by Eritja et al. using a monoprotected (O^6-*p*-nitrophenyl ethanol) xanthine phosphoramidite (*15*). In our hands, monoprotected (O^6) xanthine phosphoramidites gave poor coupling yields (~30%). MALDI-TOF analysis of oligonucleotide T3 prepared by the method of Eritja et al. was consistent with the presence of xanthine. Formic acid hydrolysis followed by RP-HPLC analysis of oligonucleotides prepared in this manner revealed the correct stoichiometric ratio of X:G:A (data not shown). However, oligonucleotides prepared via this route were observed to be unstable during storage, undergoing cleavage at X-substituted sites.

We suggest that unprotected O^2 of xanthine competes as a nucleophile with 5′-OH during the X phosphoramidite coupling step, resulting in base coupled product as shown in Figure 3. This material would be expected to be labile at xanthine owing to the hydrolytic propensity of aromatic phosphates. The HPLC peak corresponding to 34-mer (T3, Figure 2), prepared via the monoprotected route, appeared to be a single species (data not shown), implying that the incorrectly coupled oligonucleotide coeluted with the desired product. In contrast, when T3 was prepared using the bis-protected phosphoramidite, coupling yields were observed to be >95%, and the resulting oligonucleotides were found to be stable under prolonged storage at neutral pH.

The synthetic strategy for the phosphoramidite described here is derived from the Van Aerschot phosphotriester synthesis (*16*), with several modifications designed to improve product yields for preparative utility in standard phosphoramidite protocols. Chromatography of **2** following sodium nitrite oxidation using the published procedure (*16*) resulted in substantial product loss in our hands. Therefore an extraction/precipitation procedure was devised for the purification of **2** which improved the yield from ~45 to 78%. Conversion of **5** to **6** was carried out in benzene in lieu of the usual solvents such as CH_2Cl_2 or THF. This facilitated the removal of insoluble triethylamine hydrochloride from the reaction. The desired pure phosphoramidite **6** was obtained in 92% yield from **5** without any chromatography. Removal of the NPE groups following oligonucleotide synthesis was accomplished using DBU/pyridine, as described (*21*). Analysis of PAGE purified X containing oligonucleotides by MALDI-TOF MS and HPLC integration of formic acid hydrolysates revealed complete deprotection of NPE groups.

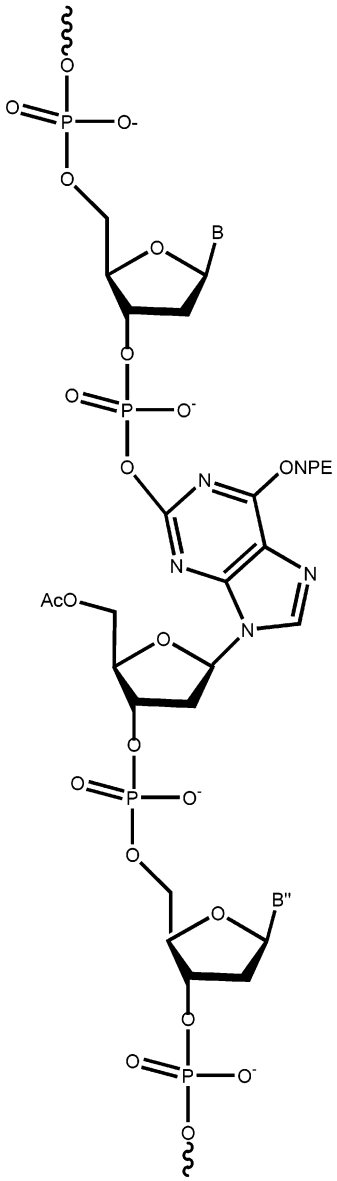

FIGURE 3: Proposed structure of the cross-coupled X containing oligonucleotide.

Stability of Xanthine in DNA. The rate constants for X depurination under a range of pH conditions were determined. Measurements were made for oligonucleotide T3 containing a uniquely substituted X at position 10. Measurement of G depurination at the corresponding position for an oligonucleotide of identical flanking sequence (T4) was carried out for comparison. These results are presented in Table 1. At pH 4, the rate of depurination of X is more than an order of magnitude greater than that determined for G within the same sequence context. Since this pH is below the pK_a for the xanthine enolate (*10*, *41*); X will be largely in the protonated form. For comparison, the corresponding enolate of G possesses a pK_a of 9.22 (*22*). At pH 5, the rate of X depurination decreases by 25-fold, while the rate for G depurination decreases by ~6-fold. Increasing the pH to 6 results in a nearly equivalent decrease in k_{obs} for both X and G, although the depurination of X is still ~4-fold faster than G. At neutral pH, the rate of depurination of X decreases even further so that it is only slightly faster than G. The ratio $k(X_{10})/k(G_{10})$ in Table 1 is ~1.2, which suggests

Table 2: Kinetic Data for dNTP Insertion on T1 and T2 Templates

enzyme	template base	incoming nucleotide	K_m (M)	k_{cat} (s^{-1})	k_{cat}/K_m ($M^{-1}\,s^{-1}$)	f_{ins}
HIV-RT	guanine	dCTP	1.63×10^{-8}	8.26×10^{-4}	5.07×10^{4}	1×10^{0}
		dTTP	5.76×10^{-5}	1.50×10^{-3}	2.61×10^{1}	5.16×10^{-4}
		dGTP	2.30×10^{-5}	8.74×10^{-4}	3.80×10^{1}	7.50×10^{-4}
		dATP	1.57×10^{-3}	4.97×10^{-4}	3.20×10^{-1}	6.25×10^{-6}
	xanthine	dCTP	1.06×10^{-4}	4.86×10^{-4}	4.58×10^{0}	1.0×10^{0}
		dTTP	6.59×10^{-5}	3.34×10^{-4}	5.07×10^{0}	1.1×10^{0}
		dGTP	2.07×10^{-4}	5.89×10^{-5}	2.8×10^{-1}	6.2×10^{-2}
		dATP	1.07×10^{-3}	9.18×10^{-5}	9.0×10^{-2}	2.0×10^{-2}
Klenow exo$^-$	guanine	dCTP	1.47×10^{-8}	7.64×10^{-3}	5.20×10^{5}	1×10^{0}
		dTTP	2.51×10^{-4}	9.91×10^{-3}	3.95×10^{1}	7.59×10^{-5}
		dGTP	6.95×10^{-5}	7.39×10^{-3}	1.06×10^{2}	2.04×10^{-4}
		dATP	2.08×10^{-4}	7.57×10^{-3}	3.64×10^{1}	7.00×10^{-5}
	xanthine	dCTP	2.45×10^{-4}	1.09×10^{-2}	4.45×10^{1}	1.0×10^{0}
		dTTP	4.65×10^{-4}	5.12×10^{-3}	1.10×10^{1}	2.5×10^{-1}
		dGTP	*a*	*a*	n/a	n/a
		dATP	*a*	*a*	n/a	n/a

[a] Below detection limits.

that under physiological conditions xanthine is stable in DNA.

Miscoding Properties of X in DNA. The coding properties of X in template DNA were examined using the Klenow fragment of *Escherichia coli* DNA polymerase 1 [Pol 1 (KF$^-$)] and the reverse transcriptase from human immunodeficiency virus (HIV-1 RT). Steady-state kinetics of incorporation of nucleoside triphosphates (dNTPs) were measured using the method of Boosalis et al. (*23*). The insertion kinetics of dNTPs were evaluated on template 39-mer oligonucleotides T1 and T2, possessing either X or G respectively at base position 16, using 5′-^{32}P end-labeled T12C oligonucleotide as primer. All steady-state kinetic parameters determined in this study are provided in Table 2. Also included are values of f_{ins}, defined as the ratio of apparent second-order rate constants for non-Watson−Crick base pairing reactions relative to the standard reaction at the same position. In the case of reactions involving template X, the standard reaction is defined by the formation of X·C base pairs. The f_{ins} value is typically less than 1 for most nonstandard base pairs although some exceptions have been recently noted (*24*).

Examination of k_{cat}/K_M values in Table 2 for the formation of X·C and G·C base pairs by the HIV enzyme reveals a difference of nearly 4 orders of magnitude. The lower efficiency of X·C base pair formation appears to be largely determined by K_M, which is 6500-fold higher. In contrast, the values of k_{cat} vary by less than 2-fold. A similar situation is observed for the corresponding PolI (KF$^-$) catalyzed reactions, where the nearly 12 000-fold greater efficiency of G·C relative to X·C base pair formation is largely due to variation in K_M.

The incorporation of any nucleotide triphosphate other than dCTP opposite X in DNA will result in a base substitution mutation. The insertion of dTTP would give rise to an apparent G to A transition. This HIV-1 RT catalyzed reaction was characterized by a k_{cat}/K_M value which was essentially the same as that observed for dCTP insertion. Discrimination by a factor of 4 against X·T in favor of X·C pairs was observed for DNA PolI(KF$^-$). The second-order rate constant for X·T base pair formation by PolI(KF$^-$) was very similar to that found for G·T base pairs ($\sim$40 $M^{-1}\,s^{-1}$). No other dNTPs except dCTP and dTTP were found to be substrates for base pairing opposite template X by this enzyme. In contrast, the HIV-1RT enzyme incorporated both purine triphosphates with an apparent second-order rate constant of 0.1−0.3 $M^{-1}\,s^{-1}$. Examination of f_{ins} values for insertion of dGTP and dATP opposite X in DNA by HIV-1 RT reveals incorporation frequencies which are 0.06 and 0.02 times that found for dCTP, respectively. These insertion frequencies may be compared to the values determined for G·G and G·A mispair formation by HIV-1 RT, which are 7.5×10^{-4} and 6.25×10^{-6}, respectively.

Recognition of X in DNA by Base Excision Repair (BER) Enzymes. To evaluate the potential for X repair in vivo by enzymes of the BER pathway, X·N containing DNA duplexes were assayed for cleavage by the Nth, Fpg, AlkA, and Mpg proteins. Duplexes were constructed by annealing the 34-mer T3 oligonucleotide to complements T5-T8 to generate the four possible X·N pairs within an identical sequence environment. Cleavage was analyzed by denaturing PAGE and integrated using a PhosphorImager. Digests with Mpg and AlkA, which possess DNA glycosylase but not AP lyase activities, were subjected to treatment with 0.2 N NaOH to generate cleavage at abasic sites. The results of these experiments are shown in Figure 4.

The percent of BER enzyme cleavage at X is also indicated in the figure. A depurination ladder (lane H) produced by treatment of T3 with 10 mM citric acid (pH 4, 70 °C, 1 h) followed by cleavage with 0.2 N NaOH is displayed in the center lane. Under these conditions, depurination occurred predominately at X10, G20, and G26. The stability of X toward hydrolysis by alkali (0.2 N NaOH, 60 °C, 30 min) is shown in lane 1. This establishes a residual background cleavage upon workup of AlkA and Mpg reactions of $\sim$1%.

The bacterial AlkA protein possessed the greatest activity for removal of X from X·C base pairs (lane 17). Approximately 52% of X was removed after 2 h of incubation with AlkA. Diminished glycosylase activity was noted toward X·T, X·G, and X·A pairs within the same sequence context. The extent of X excision by AlkA was similar for non-X·C pairs ($\sim$10%). The human homologue of AlkA, the methyl purine glycosylase (Mpg) demonstrated greater specificity for X in X·C pairs, with an observed excision efficiency of $\sim$15% (lane 7). No significant cleavage above background could be detected for X·T, X·G, or X·A pairs.

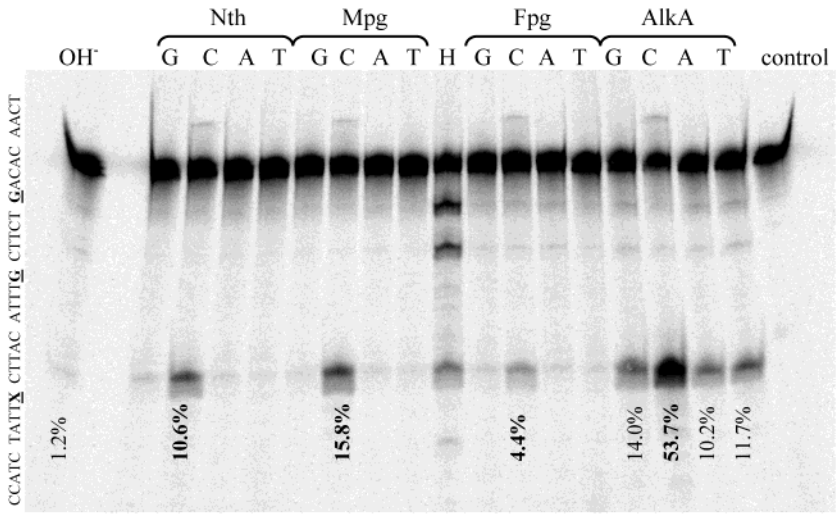

FIGURE 4: Excision of X from oligonucleotide duplexes formed from T3 and complements T5-T8 by BER enzymes. Percentages indicate the excision efficiency after 2 h incubation with the indicated BER enzymes. The H lane is a hydrolysis ladder generated by incubating T3 at 70 °C at pH 4 for 1 h. Identity of the labilized purines in the T3 sequence is indicated. The lability of X toward alkali (0.2 N NaOH, 60 °C, 30 min) is shown in lane 1.

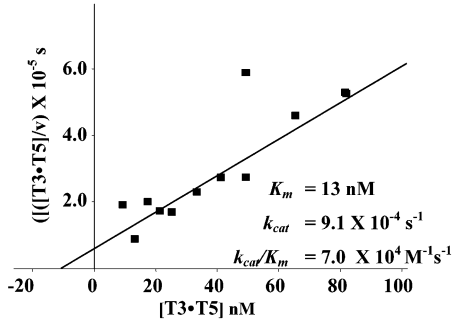

FIGURE 5: A Haynes plot for the excision of X from oligonucleotide duplex T3•T5 by the Mpg protein.

Similar specificity for X excision was also observed for the Nth and Fpg proteins, with efficiencies of ~9 and 3%, respectively. Although the activity of the Fpg enzyme toward the X•C substrate was barely above background, specificity for the "correct" base pair can be clearly observed. The steady-state kinetics of X removal by the Mpg protein were determined, and the results of a typical Hanes plot are presented in Figure 5 for the reaction with the T3•T5 duplex. The K_M of the reaction was in the nanomolar range, while the turnover number was observed to be $\sim 10^{-3}$ s^{-1}.

DISCUSSION

The important role of nitrosative deamination in NO•-mediated mutagenesis prompted a reinvestigation of some of the biochemical properties of X in DNA. Although the significance of X in DNA has been questioned due to concerns about potential instability (*25*), quantitation of this base in NO•-treated DNA (*7*, *26*, *27*), as well as mutagenic studies of NO•-treated reporter plasmids (*28*, *29*), have suggested otherwise. Synthesis of X containing oligonucleotides using the monoprotected xanthine phosphoramidite as originally described by Eritja et al. (*15*) proved problematic in our hands, consistent with what was reported by Van Aerschot et al. for the analagous phosphotriester. We therefore modified their strategy for the synthesis of the O^2,O^6 bis protected phosphotriester of xanthine for application to phosphoramidite synthesis. Oligonucleotides containing X were obtained with good coupling yields and were observed to be stable upon storage at neutral pH when prepared using the bis-protected phosphoramidite. Xanthine in DNA was found to be unstable only under acidic conditions, consistent with depurination occurring via the protonated base. At neutral pH, the enolate of X was found to depurinate with a rate constant comparable to that determined for guanine within the same sequence context. This persistence implies a role for X in mutagenesis under physiological conditions. Suzuki et al. reported that X in $d(T_5XT_6)$ underwent depurination at a rate which was ~40-fold greater than for G within the same sequence context at pH 4 at 70° C (*13*). This is ~3-fold greater than the ratio k(X)/k(G) determined in our studies, a difference that may be attributable to the different sequence contexts. Depurination rates for X at neutral pH were not determined in the studies of Suzuki et al.

The steady-state kinetics of dNTP incorporation opposite X in DNA were determined using HIV-1RT and DNA PolI(KF^-) from *E. coli* as representative polymerases. The formation of X•C base pairs by either polymerase was substantially less efficient than G•C base pair formation. The formation of alternative pairs, with the exception of HIV-1RT-catalyzed insertion of dTTP, was generally achieved with even lower efficiencies (Table 2). This suggests that X in DNA may partially inhibit replication by polymerases. The similarity of k_{cat} values for G•C and X•C base pair formation by either polymerase (<2-fold variation) suggests that some kinetic event other than polymerase dissociation is responsible for the large difference in the observed second order rate constants. Generally for polymerases, steady-state values of k_{cat} describe the rate-limiting step of enzyme dissociation from the primer/template complex (*30*). Discrimination could occur at the level of dNTP binding to the enzyme/primer/template, the covalent bond forming step, or some combination of these. Pre-steady-state kinetic experiments are in progress to distinguish between these possibilities.

Although the formation of nonmutagenic X•C base pairs is preferred for both polymerases relative to other arrange-

ments, the formation of X·T pairs occurs with comparatively high frequency. This event would give rise to an apparent G to A transition. The insertion frequency values (f_{ins}) for formation of this base pair by HIV-1 RT was found to be 1, i.e., identical to that observed for X·C pairs. For DNA PolI(KF$^-$), this value was 0.25, meaning that at equimolar dCTP and dTTP concentrations, one dTTP will be inserted opposite X in template DNA for every four dCTP incorporation events. This frequency of mispairing by PolI(KF$^-$) closely resembles that observed for mutagenic insertion of dATP opposite 8-oxoG by this enzyme (*42*). These values may be compared to f_{ins} values for dTTP incorporation opposite G, which was observed to be 5.2×10^{-4} for HIV-1 RT and 7.6×10^{-5} for DNA PolI. This corresponds to one dTTP incorporation event for every 1900 and 13 000 Watson−Crick pairs for HIV-1 RT and DNA PolI, respectively.

The published NO•-induced mutation spectra are consistent with the predominant formation of X·T base pairs at sites of guanine mutations. Treatment of the pSP189 shuttle vector with NO• gas followed by transfection into either human or bacterial cells revealed a mutation spectrum consisting nearly exclusively of G·C to A·T and A·T to G·C transitions (*28*). The deamination of C to yield uracil could in principle contribute to the G·C to A·T transitions observed in NO•-treated plasmids. However, transformation of NO•-treated DNA into an ung$^-$ *E. coli* strain did not result in a substantial increase in mutations, inconsistent with the formation of uracil (*34*). Moreover, the rate of C deamination by NO• has been reported to be at least 2-fold lower than G (*26*). These observations, in conjunction with the polymerase data reported here for dNTP insertion opposite X in DNA templates, support the hypothesis that the replicative formation of X·T pairs in NO•-treated DNA is the likely source of G to A transition mutations. Nitrosative deamination of A yields hypoxanthine (inosine), which overwhelmingly favors base pairing with C for both thermodynamic and kinetic reasons (*19*, *31*−*33*). This would yield apparent A·T to G·C transitions.

Our dNTP insertion data differ somewhat from that reported by Eritja et al. who used Drosophila DNA polymerase α to probe preferred pairing partners for template X in DNA (*15*). Insertion preference decreased in the order T > C ≫ A ≈ G with this polymerase. The preferences we observed for HIV-1RT were C ≈ T > G > A, whereas for DNA PolI(KF$^-$) we found that C > T, with no discernible incorporation of either dATP or dGTP. To some extent, variation in the insertion preferences must be attributable to the different specificities of the polymerases and the different template sequences studied. However, direct comparison with the data obtained for the Drosophila enzyme is also confounded by the possibility that the template may contain some fraction of incorrectly coupled oligomer (Figure 2).

Xanthine was observed to be a substrate for several enzymes of the BER pathway. The strongest activity was noted for the AlkA protein of *E. coli*. In all cases, X·C pairs were recognized preferentially, and only in the case of AlkA was some weak activity detected toward other X·N combinations (Figure 4). This specificity for X·C pairs recalls the activity of Fpg (MutM) protein, which preferentially excises 8-oxo-G paired with C over other combinations (*35*). The steady-state kinetic values obtained for excision of X (Figure 4) are similar to those observed for the removal of various modified bases by AlkA and Mpg proteins (*20*, *36*−*39*). This suggests that X may be a natural substrate in vivo. Characteristic steady-state kinetic features of Mpg reactions appear to be low K_M values (nM) accompanied by slow rates of product release (low k_{cat}). Other workers have recently reported excision of X in DNA by *E. coli* endonuclease V (*40*); however, no strong specificity for X·C pairs was observed. Whether X is a substrate for either the mismatch or nucleotide excision repair systems is not known. Redundancy in the repair pathways for X may suggest an evolutionary imperative for its removal, perhaps as a part of a defense mechanism against NO•-induced mutations.

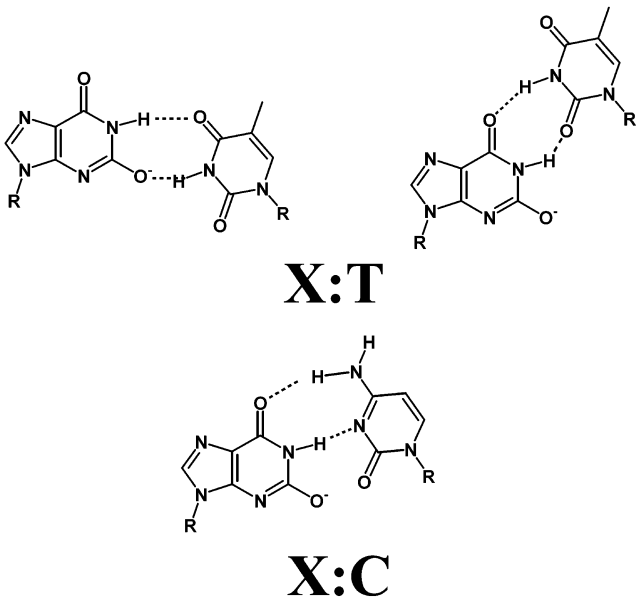

FIGURE 6: Potential arrangements for X·Pyr base pairs in antiparallel DNA duplexes involving the enolate at physiological pH.

To date, no structures of xanthine containing DNA duplexes have been determined by X-ray crystallography or NMR, thus the role of the enolate oxygen in base pairing is unknown. It might appear that this additional negative charge may act to destabilize helix formation. Physical studies of polyxanythylic acid [poly(X)] have provided support for a four-stranded structure at neutral pH. The strong alkali metal ion dependence observed for this structure suggests that the enolate helps assemble the quadraplex via metal chelation, in a manner reminiscent of other four stranded nucleic acid complexes (*41*). Evidence has also been presented for poly(X)·poly(U) four-strand helices (*11*). Some possible base pairing arrangements for X·C and X·T base pairs in an antiparallel duplex are presented in Figure 6. Whether alkali-metal ions participate in stabilizing X containing duplexes is unknown. Metal ion binding may help minimize unfavorable interactions between the O^2 carbonyl of C and the O^2 enolate of X in X·C base pairs. A role in the stabilization of hydrogen bonding involving the enolate oxygen is another possibility.

ACKNOWLEDGMENT

We would like to thank Mohammed Bouziane and Feng Miao for experimental assistance in the early part of this work, and Dr. Allan Kershaw for NMR spectra of **6**.

SUPPORTING INFORMATION AVAILABLE

^{1}H NMR spectra of **5** and **6**, ^{31}P NMR spectra of crude **6**, and MALDI-TOF mass spectrometry of xanthine containing oligonucleotides. This material is available free of charge via the Internet at http://pubs.acs.org.

REFERENCES

1. Shapiro, R., and Klein, R. S. (1966) *Biochemistry 5*, 2358−2362.
2. Lindahl, T., and Nyberg, B. (1974) *Biochemistry 13*, 3405−3410.
3. Shen, J. C., Rideout, W. M., 3rd, and Jones, P. A. (1994) *Nucleic Acids Res. 22*, 972−976.
4. Frederico, L. A., Kunkel, T. A., and Shaw, B. R. (1990) *Biochemistry 29*, 2532−2537.
5. Karran, P., and Lindahl, T. (1980) *Biochemistry 19*, 6005−6011.
6. Kosaka, H., Wishnok, J. S., Miwa, M., Leaf, C. D., and Tannenbaum, S. R. (1989) *Carcinogenesis 10*, 563−566.
7. Wink, D. A., Kasprzak, K. S., Maragos, C. M., Elespuru, R. K., Misra, M., Dunams, T. M., Cebula, T. A., Koch, W. H., Andrews, A. W., Allen, J. S., and et al. (1991) *Science 254*, 1001−1003.
8. Suzuki, T., Ide, H., Yamada, M., Endo, N., Kanaori, K., Tajima, K., Morii, T., and Makino, K. (2000) *Nucleic Acids Res. 28*, 544−551.
9. Glaser, R., Rayat, S., Lewis, M., Son, M.-S., and Meyer, S. (1999) *J. Am. Chem. Soc. 121*, 6108−6119.
10. Kinjo, Y., Tribolet, R., Corfu, N. A., and Sigel, H. (1989) *Inorg. Chem. 28*, 1480−1489.
11. Roy, K. B., and Miles, T. H. (1983) *Nucleotides Nucleosides 2*, 231−242.
12. Friedkin, M. (1952) *J. Am. Chem. Soc. 74*, 112−115.
13. Suzuki, T., Matsumura, Y., Ide, H., Kanaori, K., Tajima, K., and Makino, K. (1997) *Biochemistry 36*, 8013−8019.
14. Moschel, R. C., and Keefer, L. K. (1989) *Tetrahedron Lett. 30*, 1467−1468.
15. Eritja, R., Horowitz, D. M., Walker, P. A., Ziehler-Martin, J. P., Boosalis, M. S., Goodman, M. F., Itakura, K., and Kaplan, B. E. (1986) *Nucleic Acids Res. 14*, 8135−8153.
16. Van Aerschot, A., Mag, M., Herdewijm, P., and Vanderhaeghe, H. (1989) *Nucleotides Nucleosides 8*, 159−178.
17. Lutz, M. J., Held, H. A., Hottiger, M., Hubscher, U., Benner, S. A. (1996) *Nucleic Acids Res. 24*, 1308−1313.
18. Cantor, C. R., Warshaw, M. M., and Shapiro, H. (1970) *Biopolymers 9*, 1059−1077.
19. Valentine, M. R., and Termini, J. (2001) *Nucleic Acids Res. 29*, 1191−1199.
20. Miao, F., Bouziane, M., and O'Connor, T. R. (1998) *Nucleic Acids Res. 26*, 4034−4041.
21. Schulz, B. S., and Pfleiderer, W. (1985) *Tetrahedron Lett. 26*, 5421−5424.
22. Smith, R. M., and Martell, A. E. (1975) in *Critical Stability Constants, Volume 2*: *Amines*; Plenum Press: New York.
23. Boosalis, M. S., Petruska, J., and Goodman, M. F. (1987) *J. Biol. Chem. 262*, 14689−14696.
24. Wuenschell, G. E., Valentine, M. R., and Termini, J. (2002) *Chem Res. Toxicol. 15*, 654−661.
25. Lindahl, T. (1993) *Nature 362*, 709−715.
26. Caulfield, J. L., Wishnok, J. S., and Tannenbaum, S. R. (1998) *J. Biol. Chem. 273*, 12689−12695.
27. Nguyen, T., Brunson, D., Crespi, C. L., Penman, B. W., Wishnok, J. S., and Tannenbaum, S. R. (1992) *Proc. Natl. Acad. Sci. U.S.A. 89*, 3030−3034.
28. Routledge, M. N., Wink, D. A., Keefer, L. K., and Dipple, A. (1993) *Carcinogenesis 14*, 1251−1254.
29. Routledge, M. N. (2000) *Mutat. Res. 450*, 95−105.
30. Reardon, J. E. (1992) *Biochemistry 31*, 4473−4479.
31. Martin, F. H., Castro, M. M., Aboul-ela, F., and Tinoco, I., Jr. (1985) *Nucleic Acids Res. 13*, 8927−8938.
32. Ohtsuka, E., Matsuki, S., Ikehara, M., Takahashi, Y., and Matsubara, K. (1985) *J. Biol. Chem. 260*, 2605−2608.
33. Hill-Perkins, M., Jones, M. D., and Karran, P. (1986) *Mutat. Res. 162*, 153−163.
34. Schmutte, C., Rideout, W. M., 3rd, Shen, J. C., and Jones, P. A. (1994) *Carcinogenesis 15*, 2899−2903.
35. Castaing, B., Geiger, A., Seliger, H., Nehls, P., Laval, J., Zelwer, C., and Boiteux, S. (1993) *Nucleic Acids Res. 22*, 2899−2905.
36. O'Connor, T. R. (1993) *Nucleic Acids Res. 22*, 5561−5569.
37. Bjelland, S., Birkeland, N. K., Benneche, T., Volden, G., and Seeberg, E. (1994) *J. Biol. Chem. 269*, 30489−30495.
38. Saparbaev, M., Kleibl, K., and Laval, J. (1995) *Nucleic Acids Res. 23*, 3750−3755.
39. Roy, R., Biswas, T., Hazra, T. K., Roy, G., Grabowski, D. T., Izumi, T., Srinivasan, G., and Mitra, S. (1998) *Biochemistry 37*, 580−589.
40. He, B., Qing, H., and Kow, Y. W. (2000) *Mutat. Res. 459*, 109−114.
41. Roy, K. B., Frazier, J., and Miles, T. H. (1979) *Biopolymers 18*, 3077−3087.
42. Lowe, L. G., and Guengerich, F. P. (1996) *Biochemistry*, *35*, 9840−9849.

BI0205597